

Scaffold Flexibility Controls Binding of Herpes Simplex Virus Type 1 with Sulfated Dendritic Polyglycerol Hydrogels Fabricated by Thiol-Maleimide Click Reaction

Boonya Thongrom, Antara Sharma, Chuanxiong Nie, Elisa Quaas, Marwin Raue, Sumati Bhatia,* and Rainer Haag*

Herpes Simplex Virus-1 (HSV-1) with a diameter of 155–240 nm uses electrostatic interactions to bind with the heparan sulfate present on the cell surface to initiate infection. In this work, the initial contact using polysulfate-functionalized hydrogels is aimed to deter. The hydrogels provide a large contact surface area for viral interaction and sulfated hydrogels are good mimics for the native heparan sulfate. In this work, hydrogels of different flexibilities are synthesized, determined by rheology. Gels are prepared within an elastic modulus range of 10–1119 Pa with a mesh size of 80–15 nm, respectively. The virus binding studies carried out with the plaque assay show that the most flexible sulfated hydrogel performs the best in binding HSV viruses. These studies prove that polysulfated hydrogels are a viable option as HSV-1 antiviral compounds. Furthermore, such hydrogel networks are also physically similar to naturally occurring mucus gels and therefore may be used as mucus substitutes.

HSV-1 uses its surface glycoprotein to bind to heparan sulfate proteoglycans (HSPG) to start the infection in host cells. Because the virus entry is primarily driven by electrostatic interactions, many drug designs have been inspired by the sulfate-dominant interactions.^[5] This deals with the problem on the long-term scale, disabling the formation of a virus-reservoir. Previously, Dey et al. fabricated sulfated dendritic polyglycerol (dPGS) nanogels as synthetic heparan sulfate mimics of a range of flexibilities as well as sizes.^[6] While all the nanogels were successful in inhibiting virus, the more flexible nanogels showed higher efficacy. Recently, our group has also published a new series of dendronized linear polysulfates as multivalent inhibitors to prevent HSV entry. However, in this case, highly flexible sulfated linear polyglycerol (IPGS)

was compared with more rigid sulfated architectures. Here also, the flexible IPGS was highly successful in intervening with the infection process, showing 295 times greater efficacy than heparin.^[7]


Recently, hydrogels are emerging as important platforms for multiple applications in the biomedical arena.^[8,9] Hydrogels are formed when macromolecules crosslink by physical or chemical means to form water-swollen networks. They have a number of characteristics which make them particularly attractive for biomedical applications. For example, due to their structural similarity to living tissues, they are highly biocompatible; moreover they are able to provide low interfacial tension with the nearby tissues in the body.^[10] They can also be non-invasively injected and fill in any required shape at the injection point.^[11] In addition to other biomedical applications, they have been used in virus-trapping and containment. Zhang et al. used glycosylated hydrogels to trap the Norovirus.^[12] Importantly, mucus hydrogels within the body, function in a similar way providing the first line of defense against pathogenic attack.^[13]

The role of scaffold flexibility for virus binding is very important, yet, macroscopic materials with different stiffness have not been studied for this application. In this paper, we extend the understanding of scaffold flexibility with polyglycerol-based hydrogels. We have designed sulfated hydrogels by a click conjugation approach. Here we have employed polyethylene gly-

1. Introduction

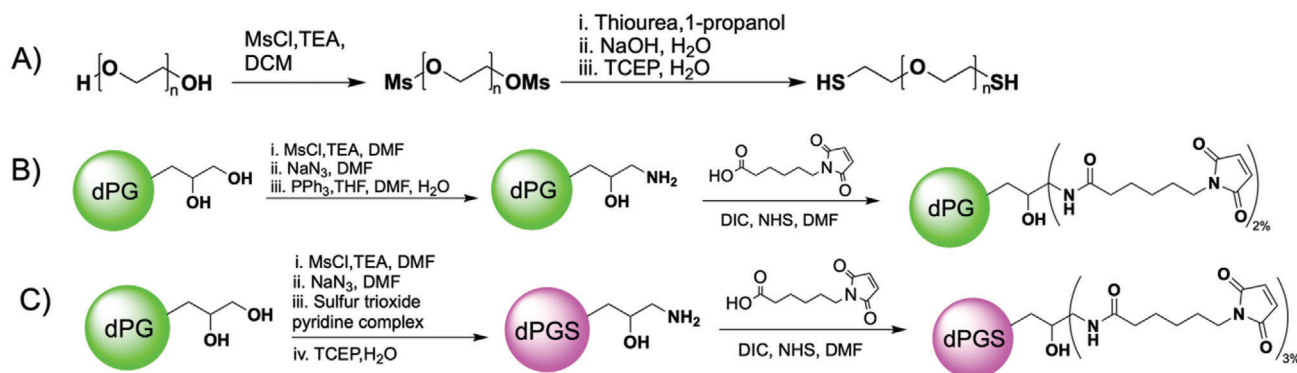
Herpes Simplex Virus-1 (HSV-1) is a part of the Herpesviridae family, which is known to target oral, pharyngeal, and genitals.^[1] The virus is supported by a wide range of hosts, including humans. HSV-1 has a high seroprevalence of $\approx 80\%$ in adults. It is an enveloped virus around 155–240 nm in diameter.^[1,2] HSV-1 can be a cause of morbidity and mortality in newborns and immunocompromised patients, and antivirals such as acyclovir (ACV) and ganciclovir are often prescribed to reduce the frequency, duration, and severity of infection.^[3,4]

B. Thongrom, A. Sharma, C. Nie, E. Quaas, M. Raue, S. Bhatia, R. Haag
Institut für Chemie und Biochemie
Freie Universität Berlin
Takustraße 3, Berlin 14195, Germany
E-mail: sumati@zedat.fu-berlin.de; haag@chemie.fu-berlin.de

 The ORCID identification number(s) for the author(s) of this article can be found under <https://doi.org/10.1002/mabi.202100507>

© 2022 The Authors. Macromolecular Bioscience published by Wiley-VCH GmbH. This is an open access article under the terms of the Creative Commons Attribution-NonCommercial License, which permits use, distribution and reproduction in any medium, provided the original work is properly cited and is not used for commercial purposes.

DOI: 10.1002/mabi.202100507



Scheme 1. Synthesis of A) PEG dithiol, B) dPG maleimide, C) dPGS maleimide.

col (PEG) dithiol and (dendritic polyglycerol sulfate) dPGS-maleimide as the macromolecular components to linear and crosslinking units, respectively. This ball-and-chain type system forms a hydrogel as a Michael-click reaction occurs between the linear PEG-dithiol and the maleimides decorating dPGs. These new sulfated hydrogels were studied by rheology and could prevent viral infection depending on the scaffold flexibility. The large surface area and highly negatively charged system allow virus binding by multivalent polyelectrolyte interactions.

2. Discussion

2.1. Design of Gel Components

We hypothesized that a ball-and-chain type polymers would further interconnect and crosslink to form a hydrogel matrix. Thus, two gel components need to be synthesized with the perspective of a facile and quick hydrogel reaction recipe. Hence, while the linear PEG “chain” component was functionalized with thiol groups, the crosslinking dPG and dPGS units were both decorated with maleimide functional groups such that the Michael addition click reaction would occur between the thiol and the maleimide units, respectively. Furthermore, in order to quantify the effect of the sulfate groups as well as to observe the individual efficacy of the matrix itself, hydrogels without sulfate, i.e., with PEG and dPG were also synthesized. These gels were then compared in separate rheology and virus binding assays.

2.1.1. Synthesis of PEG Dithiol

Commercially available PEG with a molecular weight of 6 kDa was first mesylated and subsequently purified by precipitation resulting in PEG(OMs)₂ in the form of a white powder. In order to synthesize PEG dithiol, PEG(OMs)₂ was first allowed to react with dithiourea, wherein the intermediate diisothiuronium PEG was formed. This was immediately followed by basic hydrolysis to finally obtain PEG dithiol, PEG(SH)₂. Tris(2-carboxyethyl) phosphine (TCEP) was added as reducing agent at this point, and purification thereafter by extraction and precipitation resulted in pure PEG(SH)₂, as confirmed by ¹H NMR spectroscopy. The synthesis is depicted in **Scheme 1A**.

2.1.2. Synthesis of dPG Maleimide

dPG was synthesized following the procedure in literature: dPG maleimide was synthesized in four steps. First of all, dPG was mesylated. To the mesylated product, sodium azide was added to form dPGN₃ following a substitution reaction. The resulting mixture containing the product was purified by dialysis. dPG amine was synthesized by the reduction of dPGN₃ with triphenylphosphine (TPP). Dichloromethane (DCM) wash and dialysis of the crude product resulted in pure dPGNH₂. This was corroborated by ¹H NMR and ¹³C NMR spectroscopy results. Finally, the amine group was reacted with the active (N-hydroxy Succinimid)NHS ester formed by the reaction of NHS and N,N-Diisopropylcarbodiimide (DIC) resulting in the formation of dPG maleimide. Pure dPG maleimide was obtained by dialysis of the crude product against water, confirmed thereafter by ¹H NMR studies. The synthetic steps are shown in **Scheme 1B**.

2.1.3. Synthesis of dPGS Maleimide

dPGS maleimide was prepared in a similar fashion to dPG maleimide, as depicted in **Scheme 1C**. dPGN₃ was synthesized in the same manner as mentioned above. To the same reaction mixture, sulfur trioxide pyridine complex was added and subsequently the crude mixture was first neutralized and then purified by dialyzing it against first brine, followed by water. The obtained product was then reduced and purified by dialysis. The consequent dried dPGS amine was obtained in the form of a yellow powder, the purity of which was determined by ¹H NMR spectroscopy. Afterward, dPG maleimide was synthesized by the reaction of dPGS amine with NHS and DIC. After purification by dialysis against water, the final product was obtained as a pale yellow powder. The synthetic purity and 84% degree of sulfation were confirmed by ¹H NMR spectroscopy and elemental analysis, respectively.

2.2. Synthesis of Gels

Two types of gel series were constructed. dPG maleimide gels, i.e., gels represented by “HG” were created from PEG dithiol and dPG maleimide. Further, to identify the importance of the decorating functional groups, dPGS maleimide gels (represented by

Table 1. Composition of different non-sulfated (HG) and sulfated (HGS) gel types depicting the amounts and ratios of the gel components (10% w/v PEG, 16% w/v dPG, and 10% w/v dPGS) used per 100 μ L volume.

Gel code	Gel type	PEG:dPG/dPGSMol ratio	Gel components volume[μ L]		Total gel volume [μ L]	Gel concentration [% w/v]
			PEG	dPG/dPGS		
HG 8%	dPG maleimide	2.5:1	48	20	100	8.0
HG 7%	dPG maleimide	2.5:1	42	17.5	100	7.0
HG 6%	dPG maleimide	2.5:1	36	15	100	6.0
HG 5%	dPG maleimide	2.5:1	30	12.5	100	5.0
HG 4%	dPG maleimide	2.5:1	24	10	100	4.0
HGS 8%	dPGS maleimide	2.5:1	34.3	45.7	100	8.0
HGS 6%	dPGS maleimide	2.5:1	25.8	34.2	100	6.0
HGS 5%	dPGS maleimide	2.5:1	21.5	28.5	100	5.0
HGS 4%	dPGS maleimide	2.5:1	17.2	22.8	100	4.0
HGS 3%	dPGS maleimide	2.5:1	12.9	17.1	100	3.0

“HGS”) were synthesized from the reaction between PEG dithiol and dPGS maleimide. The synthetic procedure was rapid and simple: the Phosphate buffer saline (PBS) solution of two gel components as well as an additional PBS were vortexed together so as to amount to a total of 100 μ L gel volume in the ratios indicated in **Table 1**. Further, the gels at 37 $^{\circ}$ C were allowed to swell for 1 h, and oscillatory rheology experiments were carried out to determine their mechanical properties and pore sizes. The ratio of the two reacting components in this case, PEG-dithiol and dPG maleimide was maintained to be the same as 2.5:1, respectively, in every gel decreasing the overall gel components concentration.

Increasing dilution of gel components allowed a decrease in the number of crosslinks, and thus gel elasticity decreased and conversely its viscosity increased, as can also be clearly visualized in **Figure 1B–E**. Initially, with an overall gel concentration of 8%, the rigidity of the HGS 8% gels (**Figure 1B**) is very high. For this reason, it maintains a quite rigid structure which does not flow within the measured time period.^[14] Spinnability or the ability of thread-formation is a unique property arising from non-Newtonian flow, where the existence of both elastic and viscous properties is an important prerequisite. As such, spinnability increases in viscoelastic compounds with an increase in viscosity.^[14] As the gel concentration decreases from 5% to 3% (**Figure 1C–E**), their viscosity increases. Gel HGS 5% (**Figure 1C**) is also quite elastic as it hardly flows when pressure is applied and quickly recoils to its previous position as pressure is removed. It does not display spinnability suggesting a very low viscous characteristic as well. Conversely gels HGS 4% and HGS 3% (**Figure 1D,E**, respectively), are both soft flowable gels. They are not able to maintain their conformation with the increasing pressure. In fact HGS 3% appears to be a viscous liquid; however, as evidenced by its very high spinnability, it maintains some elasticity and thus its network structure as well.

2.3. Oscillatory Rheology

A substance’s viscoelastic properties are essentially indicative of its mechanical properties and can be determined by oscillatory rheology experiments. A strain-sweep test was carried out over

the entire series to establish the linear viscoelastic region (LVE) so that consecutive oscillatory rheology experiments would be conducted in this region. These viscoelastic experiments allowed the deduction of the storage modulus, G' and the loss modulus, G'' as a function of the radial frequency, ω . Moreover, the experiments were conducted at 25 $^{\circ}$ C and at the physiological temperature 37 $^{\circ}$ C, where the viscoelastic properties of the swollen gels were measured as well. The results of the experiments at 37 $^{\circ}$ C are shown in **Figure 2**, while the results of the swollen gels are shown in **Figure 3**.

The rheological behavior of the non-sulfated gels “HG” is shown in **Figures 2A and 3A** at 37 $^{\circ}$ C in the initial and swollen states after 1-h incubation with excess water, respectively. All the gels displayed notable elastic-dominated behavior, thus providing ample proof of the stability of the crosslinks. In **Figure S8** (Supporting Information), the behavior of these gels at 25 $^{\circ}$ C can be seen. The difference caused by the increase in temperature to the physiological temperature is negligible. Interestingly, the swollen state causes a notable difference in the viscoelastic behavior in all these gels. As can be seen in **Table 2**, there is a general trend of decrease in the elastic character of this gel as the gels become more swollen.

The viscoelastic behavior of the sulfated “HGS” gels at 37 $^{\circ}$ C is shown in **Figures 2B and 3B** while their behavior at 25 $^{\circ}$ C can be seen in **Figure S9** (Supporting Information). All gels in this series can be seen to behave in a similar fashion. An increase in both moduli is seen for all cases with increasing frequency, as expected. Further, as with the HG series, all HGS gels are elastic-dominated, indicating the existence of permanent crosslinking in a solid gel matrix. In comparison to the non-sulfated HGs, the general trend of elasticity was more toward the lower end. This can be explained by the electrostatic repulsion present within these gels contributed by the sulfate groups. An increase in temperature from 25 to 37 $^{\circ}$ C did not affect the rheological properties in this case. However, a significant decrease was observed in the elastic modulus of all the sulfated gels when they were in the swollen state, as can be seen in **Table 2**. This occurs due to the increase in the general pore size with swelling and this affect is particularly pronounced due to the high-water attraction of charged sulfate groups, exemplified by gel HGS 4% wherein more than 2

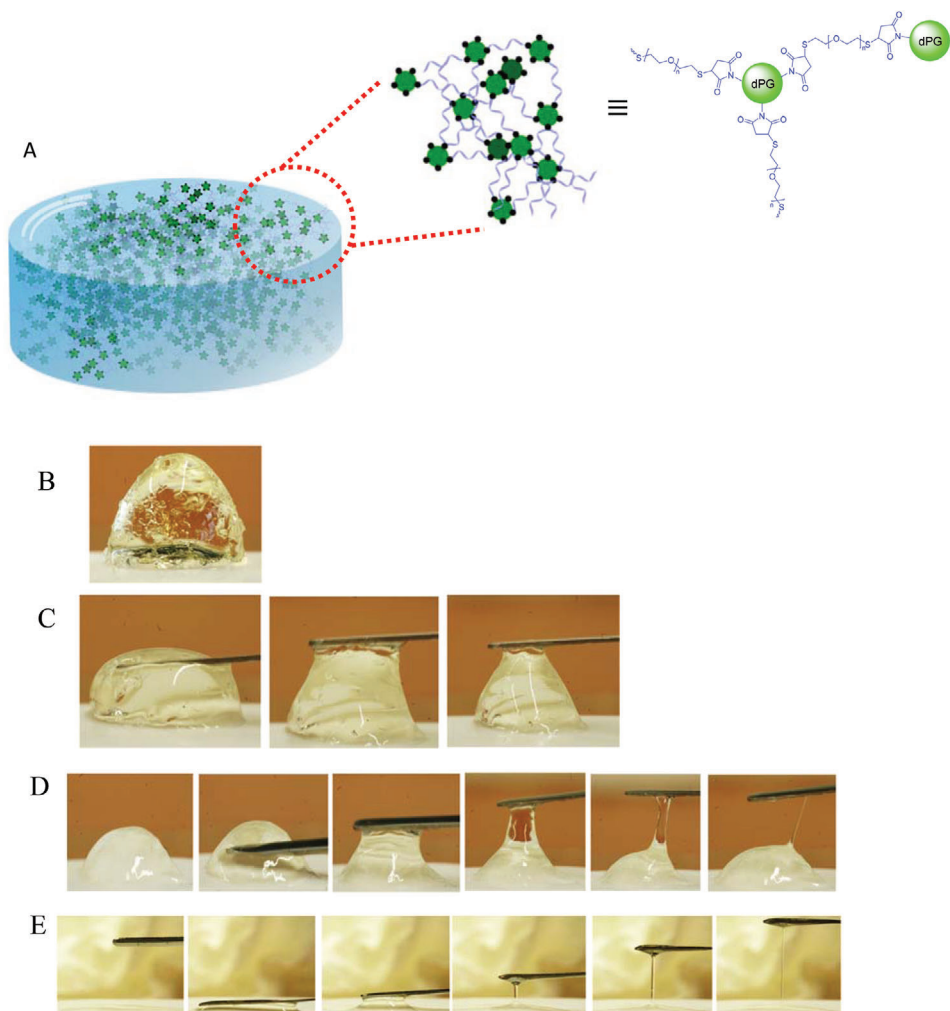


Figure 1. A) Pictorial representation of the hydrogel and its internal matrix structure (inset). The dPG units (green) are decorated with maleimide groups (black) which then react with PEG dithiol (blue) in a Michael-click reaction to result in the formation of the hydrogel. Sulfated gels B) HGS 8%, C) HGS 5%, D) HGS 4%, E) HGS 3%. Each gel displays a clear difference in its physical properties, which are dependent upon its rheological properties. Gel HGS 8% maintains a firm structure, while the viscous trait dominates in gel HGS 3%.

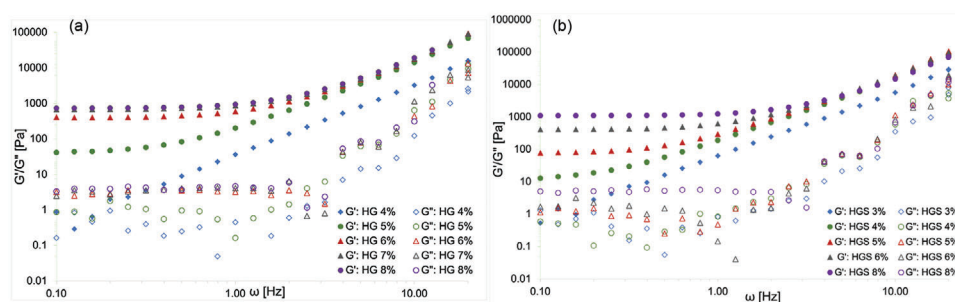


Figure 2. Storage (G') and loss (G'') moduli as a function of radial frequency (ω) of A) HG gels and B) HGS gels at 37 °C, for samples in which the gel component ratios were varied systematically.

times decrease of the elastic modulus was observed in the swollen state comparison to the initial state at 37 °C. Moreover, the change in the viscoelastic properties is more distinct in this case in comparison to the non-sulfated gels. Out of all the sulfated hydrogels, the HGS 3% was the most viscous, with its shear modulus in the

non-swollen state being only 10 Pa. The rheological behavior of the non-swollen HGS 3% network was consistent with the rest of the hydrogels in the series. For most part the elastic modulus remained higher than the viscous modulus, except for in the lower frequency range in the very beginning, as shown in Figure 2B.

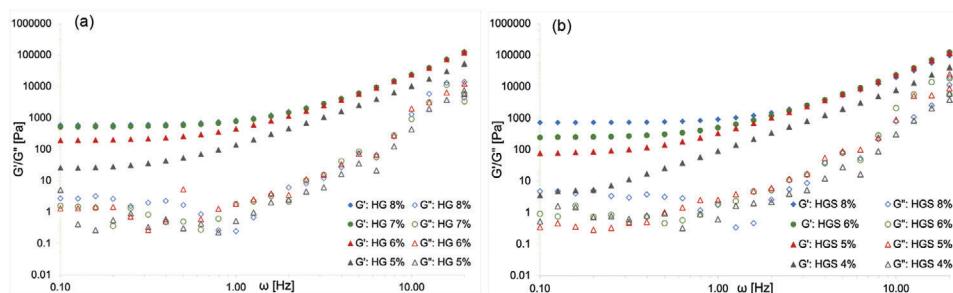


Figure 3. Storage (G') and loss (G'') moduli as a function of radial frequency (ω) of A) swollen HG gels and B) swollen HGS gels at 37 °C, for samples in which the gel component ratios were varied systematically. Gels HG 4% and HGS 3% could not be measured in a swollen state as they were too viscous and miscible when more water was introduced.

Table 2. Shear modulus G_0 and estimated mesh size of hydrogel series HG and HGS in the initial and swollen states at 37 °C.

Hydrogel ^{a)}	37 °C (Initial state)		37 °C (Swollen state)	
	Shear modulus [G_0 Pa ⁻¹]	Mesh size [ξ nm ⁻¹]	Shear modulus [G_0 Pa ⁻¹]	Mesh size [ξ nm ⁻¹]
HG 4%	5	91	–	–
HG 5%	67	39	43	46
HG 6%	433	21	234	26
HG 7%	716	18	556	19
HG 8%	766	18	630	19
HGS 3%	10	76	–	–
HGS 4%	40	47	17	62
HGS 5%	111	33	118	33
HGS 6%	442	21	283	24
HGS 8%	1119	15	748	18

^{a)} Initial state refers to the hydrogel as soon as it forms after mixing, and swollen state refers to the hydrogel after 1 h of incubation with excess water.

The existence of a stable network was also seen by spinnability. As with all other gels in this series, it is expected that its shear modulus would decrease further with swelling. For this reason, its behavior in the swollen state could not be determined, as the viscosity of the gel was quite high and therefore became miscible on the addition of PBS. However, the nature of the crosslinks remained stable as the swollen gels showed spinnability as well. In fact, the HGS 3% also show some similarities to naturally occurring gel mucus. As their shear modulus in the swollen state would be lower than 10 Pa, they would be in the approximate shear modulus range of healthy lung mucus, which is about 1–2 Pa.^[15] Moreover, lung mucus also exhibits a similar rheological pattern, maintaining a plateau at lower frequencies, and then an increase above 10 Hz.

The plateau modulus is the frequency range wherein an overall linear behavior of the storage and loss moduli is seen. Materials like hydrogels possess a complex rheological profile owing to the presence of a defined internal structure. While the macrorheology, or its bulk rheological properties such as viscoelasticity govern its functions such as lubrication and interaction with surfaces, its microrheological properties determine the diffusion behavior of small components like pathogens or drugs, within the

hydrogel matrix. While a larger mesh size allows free diffusion of a smaller component, when the two are comparable, steric hindrance on movement becomes significant. Thus precise control over the mesh size is pertinent to its application.^[16] In order to calculate the mesh size, the G' value at 0.3 Hz frequency was chosen and then substituted in the simplified equation $G' = kT/\xi^3$, where k is the Boltzmann constant, T is the temperature, and ξ is the mesh size.^[17–19] As a rule, mesh sizes increase as the crosslinking density is decreased.^[20] The lowest mesh sizes would therefore be predicted as corresponding to the least elastic hydrogel. Indeed, among the initially formed sulfated and non-sulfated hydrogel HG 4% and HGS 3% had the largest mesh size at ≈ 91 and 76 nm, respectively owing to the low crosslinking density. It was found that HSV measuring 180 nm in size were slowed down in mucus with mesh size of ≈ 100 nm, with up to a 1000-fold decrease in compared to water.^[21] The mesh size of the sulfated HGS 3% and 4% gels approaches this and can therefore be considered as suitable candidates for hindering HSV.

2.4. Cytotoxicity Studies

The cytotoxicity tests of gel components were performed against different cell types with CCK-8 kit. The Vero E6 (Figure 4A) was used, generally applied for infection assays and virus propagation studies. Moreover, the human lung cell lines A549 and HBE were also employed to diversify the study (Figure 4B,C, respectively). A slight decrease in the cell viability was observed with the addition of sulfated compounds, as expected. A high tolerance of the gel components for all the cell lines was observed, and the tolerance of dPGS decreased only at the concentration >1 mg mL⁻¹. dPG maleimide showed high cell viability throughout the tested range for all cell lines. A549, Vero E6, as well as the HeLa cell lines were treated with PEG dithiol and a high tolerance was noted in every case. These results are shown in Figure S10 (Supporting Information). Overall, all the experiments proved a high tolerance for all the gel components involved rendering them safe to be applied for future treatments.

2.5. Binding of HSV

The HSV-1 binding of the hydrogels was established by plaque reduction assays. For this purpose, the hydrogel was initially incubated with the virus solution with moderate shaking for 1 h.

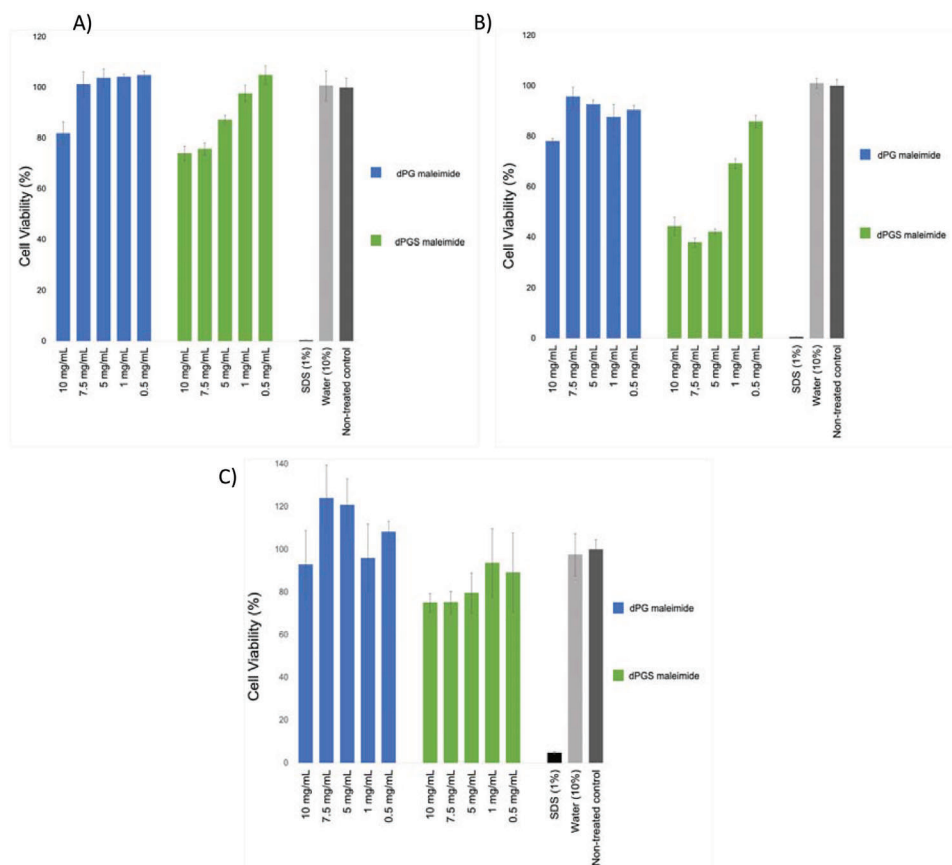


Figure 4. Cytotoxicity tests were conducted for the components of both hydrogel series, dPG-maleimide and dPGS-maleimide, as shown in A) Vero-E6 cell line, B) A549 cell line, and C) HBE cell line. For each case, the presence of sulfate groups on the gel negatively affected the cell viability results.

Afterward, the number of viral particles in the supernatant is titrated by plaque assays on Vero E6 cells. The binding with virus was revealed by reduced virus titer in the supernatant as shown in **Figure 5**.

We did not observe any significant reduction in the HSV titer with the non-sulfated control gels or gel component dPG-maleimide. The sulfated gel types (HGS 8%, HGS 6%, HGS 5%, HGS 4%, HGS 3%) showed much higher binding abilities of up to 30 times higher than their non-sulfated counterparts. HSV viruses electrostatically bind with heparan sulfate on the host cells through their surface glycoprotein. Due to the presence of sulfate groups in the HGS gels, virus binding became significantly more efficacious in comparison to HG gels. This was observed not only for every hydrogel but also for the individual sulfated and non-sulfated gel components (dPG-maleimide and dPGS-maleimide). However, as the gels HGS 8%–5% are quite stiff, their sulfate groups are less exposed even after swelling, and thus do not interact with as many HSV particles as the softer gels would. This has a negative effect on their binding performance, as can be seen in **Figure 5**. The effects of network structure on virus binding were revealed by the comparison among sulfated hydrogels with different stiffness. The more viscous gel HGS 3% being slightly better than the HGS 4%, showed a higher HSV interaction than the more elastic gels HGS 5%–8% in the series. The remaining virus titer in the supernatant treated with HGS

3% gel was 560 PFU mL⁻¹ whereas for HGS 8%, the remaining virus titer was still 1483 PFU mL⁻¹. The loosely bound network in the more flexible sulfated hydrogels might allow the exposition of more sulfate groups while binding with the virus and thus is definitely a plus for HSV binding and inhibition.

Sulfated hydrogels HGS were compared with the 2.3×10^{-3} M sulfated gel component dPGS-maleimide ($\approx 4.6\%$ w/v). As can be seen in Table S1 (Supporting Information), the concentration of sulfated gel component in the HGS 4% ($\approx 1.1 \times 10^{-3}$ M dPGS) and HGS 3% ($\approx 0.9 \times 10^{-3}$ M dPGS) are 2–2.5 times lower and all sulfate groups are not fully exposed because of 3D network formation, still the performance of these gel types were slightly higher than the dPGS-maleimide itself because of large contact surface area with the virus and high flexibility.

Thus, sulfated gels proved to be the most compelling candidates for HSV-1 binding. Moreover, the network structure also played a significant role in this study, where higher flexibility allowed higher binding capacity.

3. Conclusion

This study demonstrates the flexibility of a sulfated hydrogels network as an important parameter for its ability to bind HSV-1 virus. In order to deduce the best candidate, polyether-based hydrogels were prepared using thiol-maleimide click chemistry

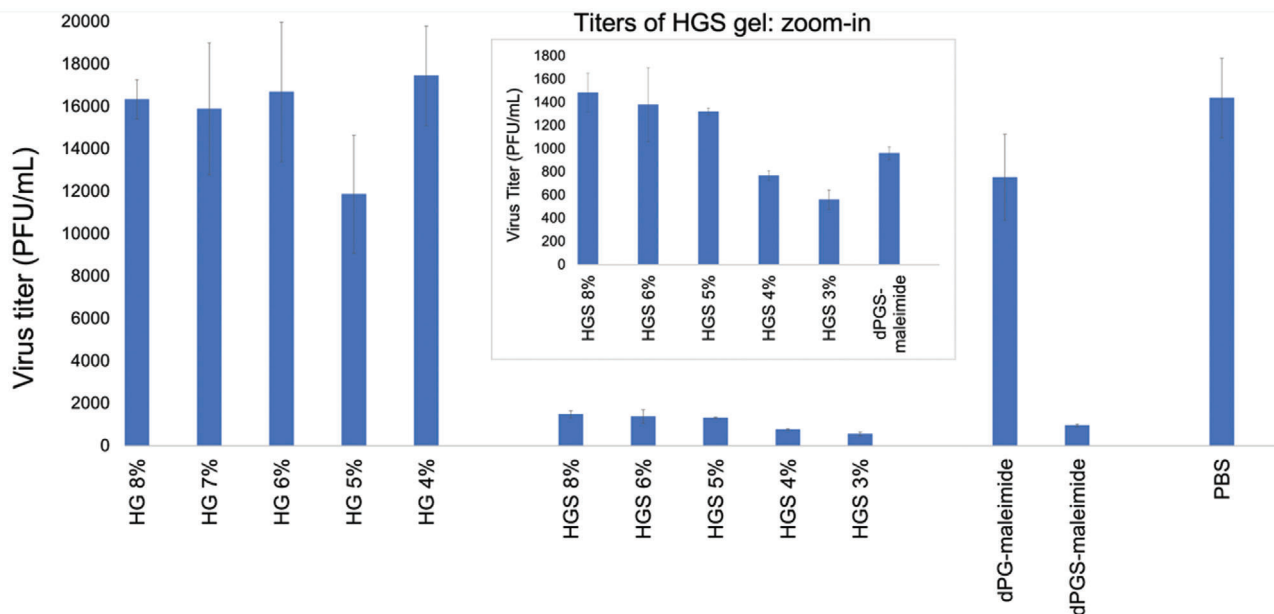


Figure 5. Efficacy of HSV-1 binding by hydrogels. The figure characterizes the virus titers after treatment with various samples. Inset: virus titers of gel series HGS, as well as dPGS-maleimide. Values are expressed as mean \pm SD, $n = 3$. dPGS-maleimide (5% w/v) and dPG-maleimide (8% w/v) were applied in the HSV binding assay.

based on dPG-maleimide as a crosslinker and PEG-dithiol as the linear component. Two sets of hydrogels were compared, distinguished by the presence of hydroxyl groups in one series and sulfate groups in the other series. Furthermore, hydrogels were prepared within each series such that their flexibility was tuned reduction of the linear component. A range of flexibilities with shear moduli between 1 and 1200 Pa were achieved. The presence of sulfate groups on hydrogels is crucial for HSV binding, rheology dependent parameters also played an important role. The sulfated hydrogels show 10–30 times stronger HSV binding than the non-sulfated controls. Furthermore, gels followed a general trend of having higher virus titer reduction as their flexibilities increased. Notably, HGS 3% proved to be the most suitable virus-binding candidate, showing an even higher binding capacity than the highly sulfated dendritic crosslinker dPGS-maleimide. These polysulfated hydrogel networks can mimic the antiviral function of mucus and may find future applications in this area.

4. Experimental Section

Materials: All chemicals were purchased from Merck KGaA, Darmstadt, Germany and/or its affiliates and used without any further purification, unless otherwise stated. The solvents used herein, i.e., diethyl ether (100%) and *N,N*-dimethylformamide (99.8%) were bought from VWR chemicals and Acros Organics, respectively, while DCM (99%) and ethyl acetate were both obtained from Fischer Scientific. Sodium hydroxide in the form of pellets, as well as in a 99.5% solution, was also procured from Fischer Scientific. Triphenylphosphine (99%) was purchased from Alfa Aesar. dPG of ≈ 6 kDa average molecular weight was prepared as previously reported^[22–24] with the improved method.^[25] For purification carried out with dialysis, Spectra Por dialysis tubing (MWCO = 2000 g mol⁻¹) (Carl Roth GmbH, Karlsruhe, Germany).

Cell viability assays were performed with a CCK-8 Kit from Sigma Aldrich according to the manufacturing instructions. A549, HBE, HeLa, and Vero

E6 cells were obtained from Leibniz-Institut DSMZ—Deutsche Sammlung von Mikroorganismen und Zellkulturen GmbH and cultured in DMEM supplemented with 10% (v/v) FBS, 100 U mL⁻¹ penicillin and 100 μ g mL⁻¹ streptomycin.

Instrumentals: The Jeol Eclipse 500 MHz (Tokyo, Japan) or a Bruker AVANCE III 700 MHz spectrometer (Billerica, MA, USA) instruments were used to measure all the NMR spectra of all the compounds (¹H and ¹³C) reported here were recorded at 300 K. Chemical shifts δ were reported in ppm and the deuterated solvent peak was used as a standard. Vario EL CHNS elemental analyzer (Elementar Analysensysteme GmbH (Langenselbold, Germany)) was used to carry out the elemental analysis of all relevant compounds reported in this work. All the rheology data reported here was measured and characterized by the Kinexus rheometer (NETZSCH GmbH, Selb, Germany). A parallel plate, 8 mm in diameter was used for all the measurements, with the average normal force maintained at ≈ 0.1 N at 25 and 37 °C. The data were analyzed by an oscillatory frequency sweep strain-controlled test with 1% strain (which is obtained from a linear viscoelastic range of an amplitude sweep test) and the reported storage modulus (G') of a rigid hydrogel were picked at 0.3 Hz.

Synthesis of Gel Components: PEG(OMs)₂: Dried PEG (20 g, 3.3 mmol, 1 eq., 6 kDa) was dissolved in a dichloromethane (DCM) solution (100 mL), and subsequently cooled down in an ice bath. Then triethylamine (TEA, 2.77 mL, 20 mmol, 6 eq.) was added to the solution, followed by the dropwise addition of methanesulfonyl chloride (1.03 mL, 13.3 mmol, 4 eq.). The reaction was allowed to run overnight. Afterward, the crude product was purified; the DCM layer was washed thrice with brine before drying it with Na₂SO₄. It was then precipitated in cooled diethyl ether. The purified precipitate was then allowed to dry overnight under vacuum, finally resulting in a white powder with 95% isolated yield. ¹H NMR: (500 MHz, CDCl₃, δ (ppm)): 3.07 (3H, s), 3.48–3.78 (m), 4.37 (2H, t) (Figure S1, Supporting Information).

Synthesis of PEG Dithiol (PEG(SH)₂): PEG(OMs)₂ (19 g, 3.2 mmol, 1 eq.) and thiourea (1.02 g, 13.3 mmol, 4 eq.) were added to a solution of 1-propanol. The solution was refluxed overnight to obtain diisothiuronium PEG as the intermediate product. Without any further purification, 1-propanol was immediately removed from the intermediate, followed by the addition of NaOH (0.53 g, 13.3 mmol, 4 eq.) and water (100 mL). The reaction mixture was allowed to reflux overnight. Afterward, tris(2-

carboxyethyl)phosphine (TCEP, 1.67 g, 6.7 mmol, 2 eq.) was added to the mixture and stirred for 2 h prior to the purification. To purify, NaCl was added to the mixture until the point of saturation, followed by the precipitation of the product was extracted three times into DCM. The DCM layer was then dried by Na₂SO₄, after which it was precipitated in cooled diethyl ether. The precipitate was dried in vacuo overnight. PEG dithiol was obtained as a pale yellowish powder in 88% isolated yield. ¹H NMR (500 MHz, CDCl₃, δ (ppm)): 1.59 (1H, t), 2.69 (2H, quat), 3.48–3.78 (m). Elemental analysis; N = 0.13; C = 54.24; S = 2.02; H = 8.47 (Figure S2, Supporting Information).

Synthesis of dPGNH₂: Dried dPG (5 g, 0.5 mmol, 1 eq.) and TEA (0.7 mL, 5 mmol, 10 eq.) were added to a solution of *N,N*-dimethyl formamide (DMF, 50 mL) and the reaction mixture was subsequently cooled using an ice bath. Methanesulfonyl chloride (0.31 mL, 4 mmol, 8 eq. to target roughly 5% mesyl groups on dPG) was added dropwise to the stirring mixture. The reaction mixture was then stirred overnight. NaN₃ (0.65 g, 10 mmol, 20 eq.) was then added to the reaction flask and thereafter heated at 60 °C for 2 days. Afterward, the crude mixture was purified in water by dialysis (MWCO = 2 kDa) for 2 days. After purification, water was first removed from the flask and DMF (40 mL) was then added to it. Separately a tetrahydrofuran (THF, 30 mL) solution of triphenylphosphine (TPP, 3.28 g, 12.5 mmol, 25 eq.) was prepared in another flask. The contents of the latter were then added gradually to the former DMF solution flask. The reaction flask was allowed to stir overnight, with additional care that phase separation did not take place. Afterward, water (5 mL) was added to the reaction mixture and stirred again overnight at room temperature overnight. Finally, the product was purified by a DCM wash, repeated three times and later dialyzed against water (MWCO = 2 kDa) for 2 days. The product obtained was then dried and collected as a pale yellowish liquid with a honey-like consistency in 70% isolated yield. ¹H NMR (700 MHz, D₂O, δ (ppm)): 0.90 (3H, broad s, initiator backbone), 1.39 (2H, broad s, initiator backbone), 2.73–4.02 (m, backbone repeating units), (Figure S3, Supporting Information). ¹³C NMR (700 MHz, D₂O, δ (ppm)): 43.07 (s, 2nd carbon next to amino group), 60.89–79.76 (m, polymer backbone) (Figure S4, Supporting Information).

Synthesis of dPG Maleimide: dPGNH₂ (1.4 g, 0.14 mmol, 1 eq.), 6-maleimidoheptanoic acid (0.15 g, 0.7 mmol, 5 eq.), and *N*-hydroxysuccinimide (0.13 g, 1.12 mmol, 8 eq.) were added to DMF (20 mL). *N,N'*-diisopropylcarbodiimide (DIC, 0.17 mL, 1.12 mmol, 8 eq.) was then added to the mixture and it was allowed to stir overnight at room temperature. The crude mixture was afterward subjected to dialysis against water (MWCO = 2 kDa) for 2 days. The purified product was later collected and kept in an aqueous solution with 85% isolated yield. ¹H NMR (700 MHz, D₂O, δ (ppm)): 0.92 (3H, broad s, initiator backbone), 1.32 (2H, broad s), 1.61 (4H, broad s), 2.28 (2H, broad s), 3.26–4.04 (m, backbone repeating units), 6.89 (2H, broad s) (Figure S5, Supporting Information).

Synthesis of dPGSNH₂: An initial mixture was made by the addition of dPG (6 g, 0.6 mmol, 1 eq.) and TEA (0.83 mL, 6 mmol, 10 eq.) were added to DMF (60 mL). The mixture was then cooled down with the help of an ice bath. Subsequently methanesulfonyl chloride (0.37 mL, 4.8 mmol, 8 eq.) was added dropwise to the stirring solution, which was then allowed to stir overnight. Following the addition of NaN₃ (0.62 g, 9.6 mmol, 16 eq.), the reaction mixture was allowed to stir as it was heated to 60 °C. After 2 days, sulfur trioxide pyridine complex (23.87 g, 150 mmol, 250 eq.) was added to the mixture and then allowed to run for 2 days at room temperature. The crude mixture was purified by first neutralizing the solution with NaOH and then dialyzing it first against brine, followed by water for 2 more days. Dialysis tubes with a 2 kDa molecular weight cut-off were used for both these cases. After purification, TCEP (1.38 g, 4.8 mmol, 8 eq.) was added to the aqueous solution and it was allowed to stir for 3 days. The crude mixture was then purified by dialysis against water (MWCO = 2 kDa) carried out for 2 days. Finally, the aqueous solution of the product was lyophilized overnight and collected as a solid pale yellow powder with 65% isolated yield with 4% as degree of sulfation. ¹H NMR (600 MHz, D₂O, δ (ppm)): 0.93 (3H, broad s, initiator backbone), 3.45–4.74 (m, backbone repeating units), elemental analysis: N 0.84, C 20.52, S 14.94, H 3.71 (Figure S6, Supporting Information).

Synthesis of dPGS Maleimide: 6-maleimidoheptanoic acid (0.07 g, 0.35 mmol, 7 eq.), and *N*-hydroxysuccinimide (0.05 g, 0.45 mmol, 9 eq.) were added to a solution of DMF (5 mL). This was followed by the addition of DIC (0.07 mL, 0.45 mmol, 9 eq.) and the mixture was stirred. After 30 min, the aqueous solution (5 mL) of dPGSNH₂ (1 g, 0.05 mmol, 1 eq.) was added to the reaction mixture and then allowed to stir overnight at room temperature. The crude product was purified by dialyzing the mixture against water with for 2 days (MWCO = 2 kDa). Finally, the aqueous solution was lyophilized and the final product was obtained as a solid, pale yellow powder in 87% isolated yield. ¹H NMR (700 MHz, D₂O, δ (ppm)): 0.94 (3H, broad s, initiator backbone), 1.30 (2H, broad s), 1.62 (4H, broad s), 2.26–2.29 (2H, broad s), 2.48–2.52 (2H, broad s), 3.40–4.75 (m, backbone repeating units), 6.93 (2H, broad s). Elemental analysis: N 1.95, C 21.75, S 16.23, H 3.62 (Figure S7, Supporting Information).

Cytotoxicity Studies: All cell experiments were conducted according to German genetic engineering laws and German biosafety guidelines in the laboratory (safety level 1). A549, HBE, and Vero E6 cells were seeded in a 96-well plate at a density of 5 × 10⁴ cells mL⁻¹ in 90 μL DMEM medium per well over night at 37 °C and 5% CO₂. 10 μL of sample (solved in deionized water) were added in serial dilutions including positive (1% SDS) and negative controls (medium, H₂O) and incubated for another 24 h at 37 °C and 5% CO₂. For background subtraction, also wells containing no cells but only sample were used. After 24 h incubation the CCK8 solution was added (10 μL well⁻¹) and absorbance (450 nm/650 nm) was measured after ≈3 h incubation of the dye using a Tecan plate reader (Infinite pro200, TECAN-reader Tecan Group Ltd.). Measurements were performed in triplicates and repeated three times. The cell viability was calculated by setting the non-treated control to 100% and the non-cell control to 0% after subtracting the background signal using the Excel software.

Virus Binding Assay: The samples were disinfected by UV-irradiation first for 30 min. Then they were incubated with HSV-1-GFP solution (300 μL, ≈20 000 PFU mL⁻¹) for 1 h with constant shaking. Afterward, the virus particles in the solution was titrated by a plaque assay on the VeroE6 line with DMEM (0.9% methylcellulose) as overlay medium. The plaques were counted after 2 days with a fluorescence microscope (Axio, Zeiss, Germany).

Supporting Information

Supporting Information is available from the Wiley Online Library or from the author.

Acknowledgements

The study was funded by the Helmholtz Graduate School of Macromolecular Bioscience, by the Deutsche Forschungsgemeinschaft (DFG, German Research Foundation)—SFB 1449—431232613; subprojects A01, B03, C04, Z02 and by the German Federal Ministry of Education and Research (82DZL0098B1). SB acknowledges the financial support by DFG-project number 458564133.

Open access funding enabled and organized by Projekt DEAL.

Conflict of Interest

The authors declare no conflict of interest.

Author Contributions

B.T. and A.S. contributed equally to this work.

Data Availability Statement

The data that support the findings of this study are available in the supplementary material of this article.

Keywords

click chemistry, HSV-1, hydrogel, polysulfates, rheology, virus binding

Received: December 13, 2021

Revised: January 24, 2022

Published online: February 23, 2022

-
- [1] P. G. Arduino, S. R. Porter, *J. Oral Pathol. Med.* **2008**, *37*, 107.
- [2] R. F. Laine, A. Albecka, S. Van De Linde, E. J. Rees, C. M. Crump, C. F. Kaminski, *Nat. Commun.* **2015**, *6*, 5980.
- [3] C. Dogramatzis, H. Waisner, M. Kalamvoki, *Viruses* **2021**, *13*, 17.
- [4] S. Crimi, L. Fiorillo, A. Bianchi, C. D'Amico, G. Amoroso, F. Gorassini, R. Mastroieni, S. Marino, C. Scoglio, F. Catalano, P. Campagna, S. Bocchieri, R. De Stefano, M. T. Fiorillo, M. Cicciù, *Viruses* **2019**, *11*, 463.
- [5] B. Ziem, W. Azab, M. F. Gholami, J. P. Rabe, N. Osterrieder, R. Haag, *Nanoscale* **2017**, *9*, 3774.
- [6] P. Dey, T. Bergmann, J. L. Cuellar-Camacho, S. Ehrmann, M. S. Chowdhury, M. Zhang, I. Dahmani, R. Haag, W. Azab, *ACS Nano* **2018**, *12*, 6429.
- [7] P. Pouyan, C. Nie, S. Bhatia, S. Wedepohl, K. Achazi, N. Osterrieder, R. Haag, *Biomacromolecules* **2021**, *22*, 1545.
- [8] H. Kamata, X. Li, U.-I. Chung, T. Sakai, *Adv. Healthcare Mater.* **2015**, *4*, 2360.
- [9] A. Herrmann, R. Haag, U. Schedler, *Adv. Healthcare Mater.* **2021**, *10*, 2100062.
- [10] B. Gyarmati, B. Vajna, Á. Némethy, K. László, A. Szilágyi, *Macromol. Biosci.* **2013**, *13*, 633.
- [11] T. J. Sanborn, P. B. Messersmith, A. E. Barron, *Biomaterials* **2002**, *23*, 2703.
- [12] Y. Zhang, Q. Yao, C. Xia, X. i Jiang, P. G. Wang, *ChemMedChem* **2006**, *1*, 1361.
- [13] R. Bansil, B. S. Turner, *Curr. Opin. Colloid Interface Sci.* **2006**, *11*, 164.
- [14] N. Tsurutaro, *Bull. Chem. Soc. Jpn.* **1952**, *25*, 88.
- [15] S. K. Lai, Y.-Y. Wang, D. Wirtz, J. Hanes, *Adv. Drug Delivery Rev.* **2009**, *61*, 86.
- [16] J. Li, D. J. Mooney, *Nat. Rev. Mater.* **2016**, *1*, 16071.
- [17] A. Sharma, B. Thongrom, S. Bhatia, B. von Lospichl, A. Addante, S. Y. Graeber, D. Lauster, M. A. Mall, M. Gradzielski, R. Haag, *Macromol. Rapid Commun.* **2021**, *42*, 2100303.
- [18] B. Von Lospichl, S. Hemmati-Sadeghi, P. Dey, T. Dehne, R. Haag, M. Sittinger, J. Ringe, M. Gradzielski, *Colloids Surf., B* **2017**, *159*, 477.
- [19] Y. Tsuji, X. Li, M. Shibayama, **2018**, *4*, 50.
- [20] K. S. Anseth, C. N. Bowman, L. Brannon-Peppas, *Biomaterials* **1996**, *17*, 1647.
- [21] S. S. Olmsted, J. L. Padgett, A. I. Yudin, K. J. Whaley, T. R. Moench, R. A. Cone, *Biophys. J.* **2001**, *81*, 1930.
- [22] H. Frey, R. Haag, *J. Biotechnol.* **2002**, *90*, 257.
- [23] A. Sunder, R. Hanselmann, H. Frey, R. Mülhaupt, *Macromolecules* **1999**, *32*, 4240.
- [24] R. Haag, A. Sunder, J.-F. Stumbé, *J. Am. Chem. Soc.* **2000**, *122*, 2954.
- [25] M. Wallert, J. Plaschke, M. Dimde, V. Ahmadi, S. Block, R. Haag, *Macromol. Mater. Eng.* **2021**, *306*, 2000688.